



## Laplace Homotopy Analysis Method to Study Fractional Non-Linear Schrodinger Equations Under Non-Singular Kernel

Vijay Kumar Regar, Hoshiyar Singh, Seema Verma and Ravi Shanker Dubey\*

**ABSTRACT:** The Schrodinger equations have various applications in quantum mechanics and physical sciences as they describe a wide range of wave propagation phenomena including dust-acoustic, Langmuir, and electromagnetic waves in plasma physics. In the present article, we employ the Laplace homotopy analysis scheme to derive exact and approximate solutions for the fractional-order Schrodinger equations under the Atangana-Baleanu derivative in Caputo sense. The significance of this work lies in extending the classical Schrödinger framework to its fractional-order counterpart by employing the ABC derivative, which possesses a non-singular and non-local kernel. By employing the proposed technique, we establish complex nonlinear fractional-order models and evaluate the efficacy by conducting numerical experiments as an application. Throughout the furnished computations, we include a comparison between the approximate values and their corresponding exact solutions, and obtain some analysis of the absolute error. The effectiveness of the proposed method is validated through numerical and graphical simulations, with results compared to established techniques such as the homotopy perturbation transform method (HPTM) and the Elzaki Adomian decomposition method (EADM). The outcome obtained confirms that the suggested approach is an alternative, straightforward, precise, and effective for solving both linear and nonlinear equations.

**Key Words:** Schrodinger equations, Atangana-Baleanu-Caputo derivative, homotopy analysis method, Laplace transform.

### Contents

<b>1 Introduction</b>	<b>1</b>
<b>2 Preliminaries</b>	<b>3</b>
<b>3 Proposed Methodology</b>	<b>3</b>
<b>4 Applications of non-linear Schrodinger equation</b>	<b>5</b>
<b>5 Results and discussions</b>	<b>9</b>
<b>6 Conclusions</b>	<b>12</b>

### 1. Introduction

The fractional Schrödinger equation has been employed to describe a variety of physical phenomena, ranging from anomalous diffusion in complex systems to the quantum behavior of particles in disordered media. The nonlinear Schrodinger equations (NLSEs), which are fundamental nonlinear evolution equations, play a crucial role in both theoretical and applied sciences. These equations are frequently used to model a wide array of physical processes, such as signal transmission through optical fibers [1,2], the propagation of electromagnetic waves in plasma physics [3], the development of rogue waves [4], and the behavior of deep-water waves in oceanic environments [5], among others.

The theory of solitons holds great importance because many models in mathematical physics exhibit soliton-like solutions. Solitons have numerous applications in mathematics and engineering. In recent years, considerable attention has been directed toward the investigation of complex optical soliton structures in nonlinear media [6,7,8,9,10,11]. Both numerical simulations and theoretical studies of the NLSEs have contributed to advancements in optical communication technologies and to a better understanding of the physical dynamics of ultra-short pulses in nonlinear and dispersive media. Laskin [12] introduced

\* Corresponding author.

Submitted July 12, 2025. Published September 29, 2025  
2010 *Mathematics Subject Classification*: 26A33, 34A08, 65H20, 65T60.

a generalized form of the classical Schrodinger equation, which governs the time evolution of quantum states and is expressed as:

$$i\kappa \frac{\partial \varphi}{\partial \eta} = \mathbb{H} |\varphi|, \quad (1.1)$$

where  $i$  is the imaginary unit,  $\kappa$  is the reduced Planck constant,  $\varphi$  is the wave function, and  $\mathbb{H}$  is the Hamiltonian operator. The Hamiltonian operator is a mathematical operator that describes the total energy of a system. Fractional Schrodinger equation of order  $\delta$  is given as [13,14].

$$i\kappa D_{\eta}^{\delta} \varphi = G |\varphi|, \quad (1.2)$$

The novelty of this manuscript lies in studying the fractional Schrödinger problem, which arises from the need to incorporate non-local and memory-dependent effects into quantum mechanics, which are not adequately captured by the classical integer-order Schrödinger equation. By employing the Atangana–Baleanu–Caputo (ABC) derivative with its non-singular Mittag–Leffler kernel, the model provides a more realistic description of diffusion, transport, and dynamical processes in complex media, ensuring that solutions remain bounded, stable, and physically consistent. The main motivation and advantage of this approach lie in its ability to unify analytical tractability with physical applicability. Furthermore, the integration of the Laplace transform with the Homotopy Analysis Method (HAM) yields efficient closed-form series solutions, offering significant computational benefits for simulating fractional quantum phenomena. Thus, the proposed model not only extends the scope of classical Schrödinger dynamics but also establishes a mathematically rigorous and physically meaningful framework.

Fractional calculus has attracted increasing attention because of its ability to model complex systems with memory and hereditary properties. It has proven effective in diverse areas such as diffusion processes, viscoelastic damping, fluid flow, quantum mechanics, heat transfer, and kinetic theory [15,16,17,18,19,20,21]. From a modeling perspective, fractional derivatives provide a powerful mathematical instrument for analyzing nonlinear dynamical systems in these fields.

Recent contributions in the field further highlight the effectiveness of fractional operators and hybrid analytical and numerical schemes in tackling complex models across applied sciences. For instance, fractional Burger equations have been analyzed using the local fractional Elzaki transform decomposition method [22], while generalized fractional derivatives have been applied to infection dynamics in SIR models [23] and rabies spread [24]. Similar approaches have been extended to cancer–virotherapy interactions [25], fractional–fractal Boussinesq equations [26], and COVID-19 transmission modeling with the Atangana–Baleanu operator [27]. Furthermore, novel hybrid and decomposition methods have been developed to address diffusion equations [28,29], Whitham–Broer–Kaup systems [30], and multi-dimensional fractional diffusion problems involving Caputo–Fabrizio derivatives [31]. These studies collectively demonstrate that fractional calculus, particularly when combined with advanced transforms, offers a versatile and robust mathematical framework for modeling real-world problems with memory and hereditary effects.

In this study, the Homotopy Analysis Transform Method (HATM) is applied to investigate nonlinear fractional Schrödinger equations under the ABC derivative. The ABC operator is particularly effective in capturing the transition from stretched exponential to power-law distributions, as well as the conversion of Gaussian to non-Gaussian behaviors. The Homotopy Analysis Method (HAM), which merges perturbation techniques with the concept of homotopy, is notable for not requiring assumptions of small or large parameters and has been successfully used in a wide range of nonlinear problems [32,33,34,35]. Moreover, methods such as the Homotopy Perturbation Method (HPM), the Adomian Decomposition Method (ADM), and the Variational Iteration Method (VIM) emerge as special cases of HAM when the convergence-control parameter is set to  $\hbar = -1$  [36,37,38]. To obtain the required analytical and graphical results, all computations were carried out using the MATLAB software package, which facilitated symbolic manipulation and visualization.

The remainder of this article is organized as follows: Section 2 presents preliminaries on fractional calculus, Section 3 introduces the basic idea of proposed technique, Section 4 provides applications, Section 5 discusses the results, and Section 6 concludes with key findings.

## 2. Preliminaries

**Definition 2.1** The usual definition of the Atangana-Baleanu-Caputo derivative (ABC) of order  $0 < \delta < 1$  is defined [39] as follows:

$${}_0^{ABC}D_\xi^\delta [f(\xi)] = \frac{\mathcal{A}(\delta)}{1-\delta} \int_0^\xi E_\delta \left( -\frac{\delta(\xi-s)^\delta}{1-\delta} \right) f'(s) ds, \quad \xi > 0, \quad (2.1)$$

where  $\mathcal{A}(\delta)$  is a normalization constant,  $E_\delta$  is the Mittag-Leffler function, and  $\Gamma(\delta)$  is the Gamma function.

**Definition 2.2** The usual definition of the Laplace Transform (LT) [40] is defined as follows:

$$\mathcal{L}\{f(\xi)\} = F(\eta) = \int_0^\infty e^{-\eta t} f(\xi) dt, \quad (2.2)$$

where  $\eta \in \mathbb{C}$  is the complex frequency parameter, and  $f(\xi)$  is a function of time  $\xi \geq 0$ .

**Definition 2.3** The Laplace Transform (LT) of the Atangana-Baleanu-Caputo (ABC) derivative of order  $0 < \delta < 1$ , is given as [39]:

$$\mathcal{L} [{}_0^{ABC}D_\xi^\delta [f(\xi)]] = \mathcal{A}(\delta) \left( \frac{s^\delta \mathcal{L}[f(\xi)](s) - s^{\delta-1} f(0)}{\delta + (1-\delta)s^\delta} \right)'. \quad (2.3)$$

**Lemma 1:** The ABC fractional integral equation for function  $f(\xi) \in H^1(0, t)$  and the non-local kernel is given as:

$${}_0^{ABC}I_\xi^\delta f(\xi) = \frac{1-\delta}{\mathcal{A}(\delta)} f(\xi) + \frac{\delta}{\mathcal{A}(\delta)\Gamma(\delta)} \int_0^\xi (\xi-s)^{\delta-1} f(s) ds. \quad (2.4)$$

For proof of the above Lemma 1, see [41].

**Lemma 2:** The ABC fractional differential equation given as

$${}_0^{ABC}D_\xi^\delta f(\xi) = g(\xi), \quad f(0) = g_0, \quad (2.5)$$

has a solution; that is [40]

$$f(\xi) = f(0) + \frac{1-\delta}{\mathcal{A}(\delta)} g(\xi) + \frac{\delta}{\mathcal{A}(\delta)\Gamma(\delta)} \int_0^\xi (\xi-s)^{\delta-1} f(s) ds. \quad (2.6)$$

## 3. Proposed Methodology

To formulate the basic idea of the proposed methodology, we consider the following nonlinear fractional partial differential equation.

$${}_0^{ABC}\mathcal{D}_\xi^\delta \varphi(\omega, \xi) + \mathfrak{R}[\varphi(\omega, \xi)] + \mathfrak{N}[\varphi(\omega, \xi)] = \phi(\omega, \xi), \quad 0 < \delta \leq 1, \quad (3.1)$$

where  ${}_0^{ABC}\mathcal{D}_\xi^\delta \varphi(\omega, \xi)$  is the ABC derivative,  $\mathfrak{N}[\varphi(\omega, \xi)]$  and  $\mathfrak{R}[\varphi(\omega, \xi)]$  are nonlinear and linear operators, respectively, while  $\phi(\omega, \xi)$  is source term.

Applying the Laplace transform to (3.1), we obtain the following.

$$\mathcal{A}(\delta) \left( \frac{s^\delta \mathcal{L}[\varphi(\omega, \xi)] - s^{\delta-1} \varphi(\omega, 0)}{\delta + (1-\delta)s^\delta} \right) + \mathcal{L}[\mathfrak{R}[\varphi(\omega, \xi)] + \mathfrak{N}[\varphi(\omega, \xi)] - \phi(\omega, \xi)] = 0. \quad (3.2)$$

Upon simplifying the above equation (3.2), we find that

$$\mathcal{L}[\varphi(\omega, \xi)] - \frac{\varphi(\omega, 0)}{s} + \left( \frac{1 + \delta(s^{-\delta} - 1)}{\mathcal{A}(\delta)} \right) \mathcal{L}[\mathfrak{R}[\varphi(\omega, \xi)] + \mathfrak{N}[\varphi(\omega, \xi)] - \phi(\omega, \xi)] = 0. \quad (3.3)$$

We define the non-linear operator as

$$N[\Upsilon(\omega, \xi; q)] = \mathcal{L}[\Upsilon(\omega, \xi; q)] - \frac{\varphi(\omega, 0)}{s} + \left( \frac{1+\delta(s^{-\delta}-1)}{\mathcal{A}(\delta)} \right) \mathcal{L}[\Re[\Upsilon(\omega, \xi; q)] + \aleph[\Upsilon(\omega, \xi; q)] - \phi(\omega, \xi)], \quad (3.4)$$

In the above equation,  $q \in [0, 1]$  is an artificial embedding parameter and  $\Upsilon(\omega, \xi; q)$  is a real function of  $\omega, \xi, q$ . Liao [32,33,34] constructed the following zero-order deformation equation:

$$(1-q)\mathcal{L}[\Upsilon(\omega, \xi; q) - \varphi_0(\omega, \xi)] = \hbar q \mathcal{H}(\omega, \xi) N[\Upsilon(\omega, \xi; q)], \quad (3.5)$$

where,  $\mathcal{H}(\omega, \xi)$  denotes a nonzero auxiliary function,  $\hbar \neq 0$  is an auxiliary parameter,  $\varphi_0(\omega, \xi)$  is the initial guess of  $\varphi(\omega, \xi)$ , and  $\Upsilon(\omega, \xi; q)$  is the unknown function. Based on the concept of HATM, one has great freedom to choose auxiliary parameter and initial guess. Obviously, when  $q = 1$ , and  $q = 0$  in (3.5), the following results hold.

$\Upsilon(\omega, \xi; 0) = \varphi_0(\omega, \xi)$ , and  $\Upsilon(\omega, \xi; 1) = \varphi(\omega, \xi)$  respectively. Thus, as  $q$  increases from 0 to 1, the solution  $\Upsilon(\omega, \xi; q)$  varies from the initial guess  $\varphi_0(\omega, \xi)$  to the solution  $\varphi(\omega, \xi)$ . Expanding  $\Upsilon(\omega, \xi; q)$  as Taylor series with respect to  $q$ , we deduce

$$\Upsilon(\omega, \xi; q) = \varphi_0(\omega, \xi) + \sum_{p=1}^{\infty} \varphi_p(\omega, \xi) q^p, \quad (3.6)$$

where,

$$\varphi_p(\omega, \xi) = \left[ \frac{1}{\Gamma(p+1)} \frac{\partial^p \Upsilon(\omega, \xi; q)}{\partial q^p} \right]_{q=0}. \quad (3.7)$$

If the auxiliary parameter  $\hbar$ , the initial guess, and auxiliary function are choosing properly, then (3.6) converges at  $q = 1$ , and

$$\varphi(\omega, \xi) = \varphi_0(\omega, \xi) + \sum_{p=1}^{\infty} \varphi_p(\omega, \xi), \quad (3.8)$$

is the solution of the original problem (3.1). Define the vectors

$$\vec{\varphi}_p(\omega, \xi) = \{\varphi_0(\omega, \xi), \varphi_1(\omega, \xi), \dots, \varphi_p(\omega, \xi)\}. \quad (3.9)$$

Differentiating (3.5)  $q$ -times with respect to  $q$  and then setting  $q = 0$  and finally dividing by  $\Gamma(p+1)$ , we have the so-called  $\mathcal{M}^{th}$ -order deformation equation

$$\mathcal{L}[\varphi_p(\omega, \xi) - \chi_p \varphi_{p-1}(\omega, \xi)] = \hbar \mathcal{H}(\omega, \xi) R_p(\vec{\varphi}_{p-1}, \omega, \xi), \quad (3.10)$$

where,

$$R_p(\vec{\varphi}_{p-1}, \omega, \xi) = \left[ \frac{1}{\Gamma(p)} \frac{\partial^{(p-1)} N[\Upsilon(\omega, \xi; q)]}{\partial q^{(p-1)}} \right]_{q=0}, \quad (3.11)$$

and

$$\chi_p = \begin{cases} 0, & p \leq 1 \\ 1, & p > 1 \end{cases}. \quad (3.12)$$

applying inverse LT to both side of (3.10), we get

$$\varphi_p(\omega, \xi) = \chi_p \varphi_{p-1}(\omega, \xi) + \mathcal{L}^{-1}[\hbar \mathcal{H}(\omega, \xi) R_p(\vec{\varphi}_{p-1}, \omega, \xi)], \quad (3.13)$$

where,

$$R_p(\vec{\varphi}_{p-1}, \omega, \xi) = ({}^{ABC}D_{\eta}^{\delta} \varphi_{p-1}(\omega, \eta)) + \Re[\varphi_{p-1}(\omega, \eta)] + \aleph[\varphi_{p-1}(\omega, \eta)] - (1 - \chi_p) \phi(\omega, \eta). \quad (3.14)$$

Finally, using (3.13), we easily compute  $\varphi_p(\omega, \xi)$  for  $p \geq 1$ , and at  $\mathcal{M}^{th}$ -order we deduce

$$\varphi(\omega, \xi) = \lim_{\mathcal{M} \rightarrow \infty} \sum_{p=0}^{\mathcal{M}} \varphi_p(\omega, \xi). \quad (3.15)$$

#### 4. Applications of non-linear Schrodinger equation

**Application 1.** Consider the nonlinear fractional Schrodinger equation [42,43,44,45]

$$i^{ABC} D_{\xi}^{\delta} \varphi + \varphi_{\omega\omega} + \Phi |\varphi|^2 \varphi = 0, \quad (4.1)$$

with the initial condition

$$\varphi(\omega, 0) = e^{i\mu\omega}, \quad (4.2)$$

where  $\Phi$  denotes potential parameter scaling in Schrödinger dynamics, and  $\mu$  is the fractional index governing memory strength in diffusion,  $|\varphi|^2 = \varphi\bar{\varphi}$ ,  $\bar{\varphi}$  is the conjugate of  $\varphi$ , and the exact solution of (4.1) for  $\delta = 1$  is  $\varphi(\omega, \xi) = e^{i(\mu\omega + (\Phi - \mu^2)\xi)}$ .

By performing Laplace transform (LT) on both sides of (4.1) and with the help of (4.2), we get

$$\mathcal{L}[\varphi(\omega, \xi)] = \frac{1}{s} (e^{i\mu\omega}) + \frac{i}{\mathcal{A}(\delta)} \left(1 - \delta + \frac{\delta}{s^{\delta}}\right) \mathcal{L} \left[ \frac{\partial^2 \varphi}{\partial \omega^2} + \Phi \varphi \bar{\varphi} \varphi \right]. \quad (4.3)$$

The non-linear operator N is presented with the help of future algorithm as below

$$N[\Upsilon(\omega, \xi; q)] = \mathcal{L}[\varphi(\omega, \xi; q)] - \frac{1}{s} (e^{i\mu\omega}) - \frac{i}{\mathcal{A}(\delta)} \left(1 - \delta + \frac{\delta}{s^{\delta}}\right) \mathcal{L} \left[ \frac{\partial^2 \varphi}{\partial \omega^2} + \Phi \varphi \bar{\varphi} \varphi \right]. \quad (4.4)$$

The deformation equation of  $p^{th}$  order by the help of HATM at  $\mathcal{H}(\omega, \xi) = 1$ , is given as follows

$$\mathcal{L}[\varphi_p(\omega, \xi) - \chi_p \varphi_{p-1}(\omega, \xi)] = \hbar R_p(\vec{\varphi}_{p-1}, \omega, \xi), \quad (4.5)$$

where,

$$\begin{aligned} R_p(\vec{\varphi}_{p-1}, \omega, \xi) &= L[\varphi_{p-1}] - (1 - \chi_p) \frac{1}{s} (e^{i\mu\omega}) \\ &\quad - \frac{i}{\mathcal{A}(\delta)} \left(1 - \delta + \frac{\delta}{s^{\delta}}\right) \mathcal{L} \left[ \frac{\partial^2 \varphi_{p-1}}{\partial \omega^2} + \Phi \sum_{r=0}^{p-1} \sum_{k=0}^r \varphi_k \bar{\varphi}_{k-r} \varphi_{p-r-1} \right]. \end{aligned} \quad (4.6)$$

On applying inverse LT to both side of (4.5), it reduces to

$$\varphi_p(\omega, \xi) = \chi_p \varphi_{p-1}(\omega, \xi) + \hbar \mathcal{L}^{-1} [R_p(\vec{\varphi}_{p-1}, \omega, \xi)]. \quad (4.7)$$

On simplifying the above equation systematically by using initial condition (4.2), we can evaluate

$$\begin{aligned} \varphi_0(\omega, \xi) &= e^{i\mu\omega}, \\ \varphi_1(\omega, \xi) &= -i\hbar [e^{i\mu\omega} (\Phi - \mu^2)] \left( \frac{1 - \delta + \delta \left( \frac{\xi^{\delta}}{\Gamma(\delta+1)} \right)}{\mathcal{A}(\delta)} \right), \\ \varphi_2(\omega, \xi) &= (1 + \hbar) \varphi_1(\omega, \xi) + \hbar^2 e^{i\mu\omega} \left( (\Phi - \mu^2) i \right)^2 \frac{1}{(\mathcal{A}(\delta))^2} \\ &\quad \times \left( 1 + 2\delta \left( 1 + \left( \frac{\xi^{\delta}}{\Gamma(\delta+1)} \right) \right) + \delta^2 \left( 1 + \left( \frac{\xi^{2\delta}}{\Gamma(2\delta+1)} \right) - 2 \left( \frac{\xi^{\delta}}{\Gamma(\delta+1)} \right) \right) \right), \end{aligned}$$

Similarly, we obtain next terms in the same manner. The approximate solution of (4.1) for  $\hbar = -1$  and  $\delta = 1$  is given as:

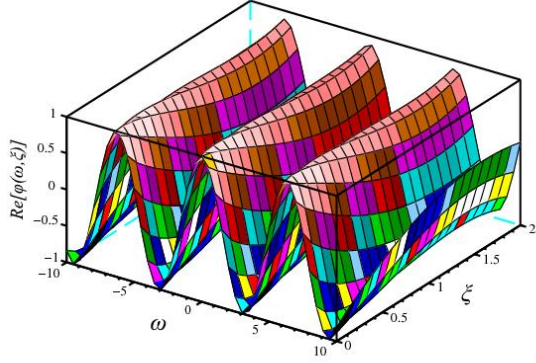
$$\begin{aligned} \varphi_{\mathcal{M}}(\omega, \xi) &= \sum_{p=0}^{\mathcal{M}} \varphi_p(\omega, \xi), \\ &= e^{i\mu\omega} \left( 1 + i(\Phi - \mu^2)\xi + (i(\Phi - \mu^2))^2 \frac{\xi^2}{2!} + \dots + (i(\Phi - \mu^2))^{\mathcal{M}} \frac{\xi^{\mathcal{M}}}{\mathcal{M}!} \right), \\ &= e^{i\mu\omega} \sum_{p=0}^{\mathcal{M}} \frac{(i(\Phi - \mu^2))^p}{p!} \xi^p. \end{aligned} \quad (4.8)$$

Letting  $\mathcal{M} \rightarrow \infty$ , we have the exact solution of (4.1) as

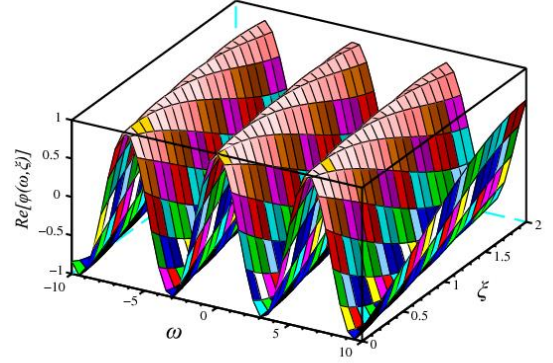
$$\begin{aligned} \varphi(\omega, \xi) &= e^{i\mu\omega} \lim_{\mathcal{M} \rightarrow \infty} \sum_{p=0}^{\mathcal{M}} \frac{(i(\Phi - \mu^2))^p}{p!} \xi^p. \\ &= e^{i(\mu\omega + (\Phi - \mu^2)\xi)}. \end{aligned} \quad (4.9)$$

Table I: The absolute error analysis between proposed method and HPTM [42] at  $\Phi = 2$ ,  $\omega = 0.2$ ,  $\mu = 1$ ,  $\delta = 1$ , and  $\hbar = -1$  for application 1.

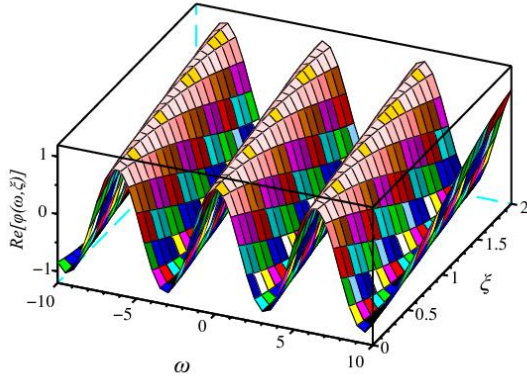
$\xi$	$\text{Re}[\varphi]_{Exact}$	$\text{Re}[\varphi]_{HATM}^{Abs}$	$\text{Re}[\varphi]_{HPTM}^{Abs}$	$\text{Im}[\varphi]_{Exact}$	$\text{Im}[\varphi]_{HATM}^{Abs}$	$\text{Im}[\varphi]_{HPTM}^{Abs}$
0.1	$9.55336 \times 10^{-1}$	$1.35702 \times 10^{-9}$	$1.35702 \times 10^{-9}$	$2.95520 \times 10^{-1}$	$2.95323 \times 10^{-10}$	$2.95323 \times 10^{-10}$
0.2	$9.21061 \times 10^{-1}$	$8.65506 \times 10^{-8}$	$8.65506 \times 10^{-8}$	$3.89418 \times 10^{-1}$	$2.01346 \times 10^{-8}$	$2.01346 \times 10^{-8}$
0.3	$8.77583 \times 10^{-1}$	$9.82114 \times 10^{-7}$	$9.82114 \times 10^{-7}$	$4.79426 \times 10^{-1}$	$2.43305 \times 10^{-7}$	$2.43305 \times 10^{-7}$
0.4	$8.25336 \times 10^{-1}$	$5.49515 \times 10^{-6}$	$5.49515 \times 10^{-6}$	$5.64642 \times 10^{-1}$	$1.44488 \times 10^{-6}$	$1.44488 \times 10^{-6}$
0.5	$7.64842 \times 10^{-1}$	$2.08672 \times 10^{-5}$	$2.08672 \times 10^{-5}$	$6.44218 \times 10^{-1}$	$5.80614 \times 10^{-6}$	$5.80614 \times 10^{-6}$
0.6	$6.96707 \times 10^{-1}$	$6.20037 \times 10^{-5}$	$6.20037 \times 10^{-5}$	$7.17356 \times 10^{-1}$	$1.82078 \times 10^{-5}$	$1.82078 \times 10^{-5}$
0.7	$6.21610 \times 10^{-1}$	$1.55526 \times 10^{-4}$	$1.55526 \times 10^{-4}$	$7.83327 \times 10^{-1}$	$4.80863 \times 10^{-5}$	$4.80863 \times 10^{-5}$
0.8	$5.40302 \times 10^{-1}$	$3.44589 \times 10^{-4}$	$3.44589 \times 10^{-4}$	$8.41471 \times 10^{-1}$	$1.11933 \times 10^{-4}$	$1.11933 \times 10^{-4}$
0.9	$4.53596 \times 10^{-1}$	$6.94386 \times 10^{-4}$	$6.94386 \times 10^{-4}$	$8.91207 \times 10^{-1}$	$2.36508 \times 10^{-4}$	$2.36508 \times 10^{-4}$
1.0	$3.62358 \times 10^{-1}$	$1.29829 \times 10^{-3}$	$1.29829 \times 10^{-3}$	$9.32039 \times 10^{-1}$	$4.62838 \times 10^{-4}$	$4.62838 \times 10^{-4}$



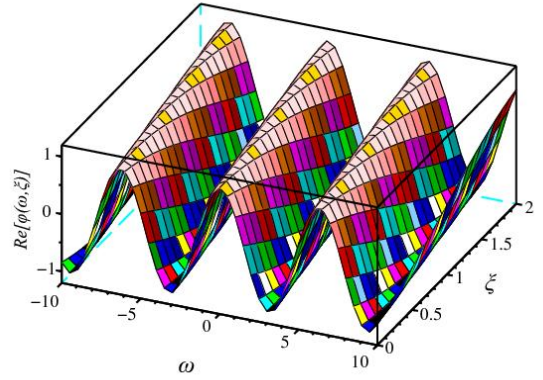
(a)  $\delta = 0.70$



(b)  $\delta = 0.90$



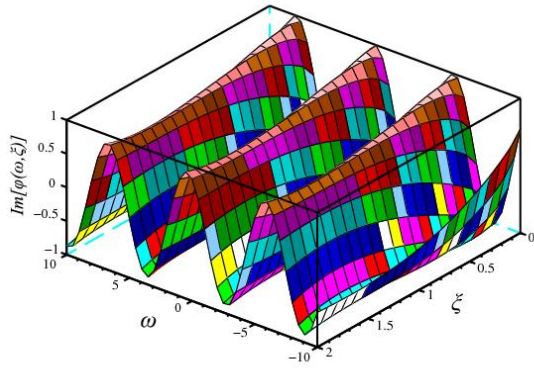
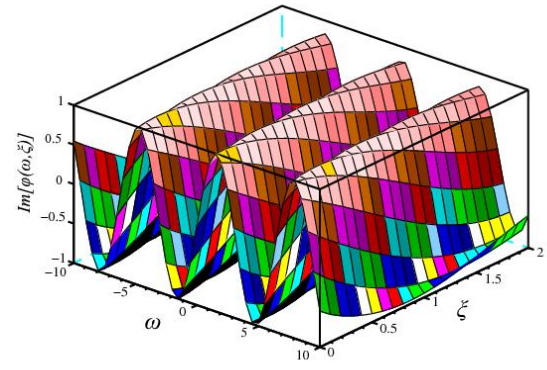
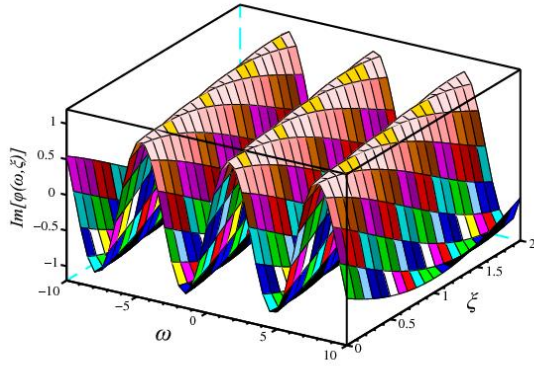
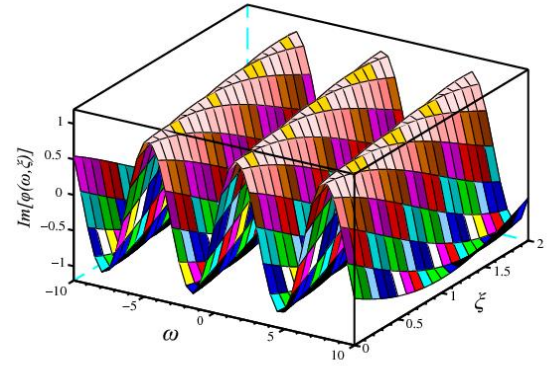
(c)  $\delta = 1$



(d) exact solution

Figure 1: 3-D behaviour of real part of application 1 for various values of  $\delta$  with  $\hbar = -1$ ,  $\Phi = 2$  and  $\mu = 1$ .



(a)  $\delta = 0.70$ (b)  $\delta = 0.90$ (c)  $\delta = 1$ 

(d) exact solution

Figure 2: 3-D behaviour of the imaginary part of application 1 for various values of  $\delta$  with  $\hbar = -1$ ,  $\Phi = 2$  and  $\mu = 1$ .

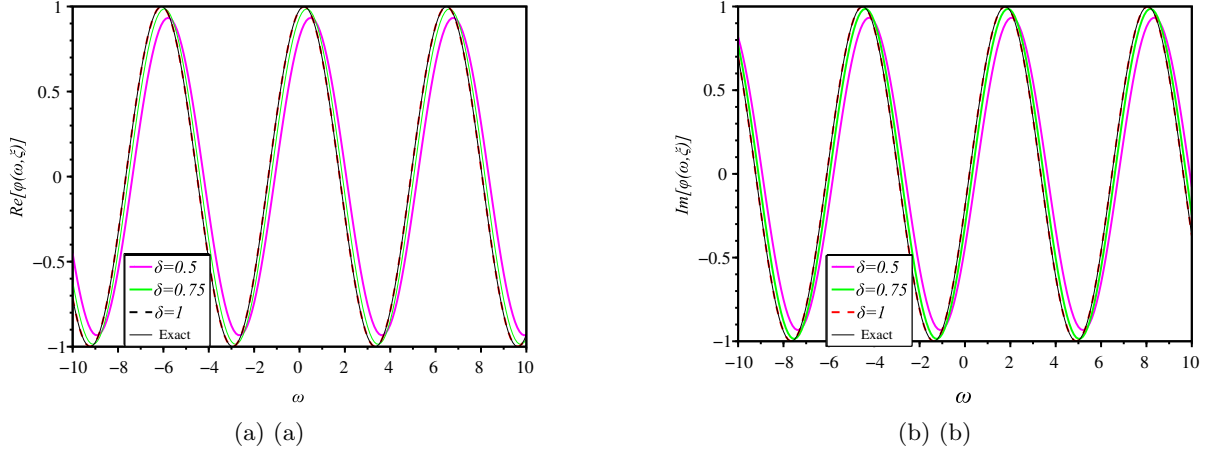


Figure 3: 2-D plots (a) real part and (b) imaginary part of application 1 for various values of  $\delta$  with  $\Phi = 2$ ,  $\hbar = -1$ ,  $\xi = 0.2$  and  $\mu = 1$ .

**Application 2.** Consider the cubic nonlinear fractional Schrodinger equation [43,44,45,46]

$$i^{ABC} D_{\xi}^{\delta} \varphi(\omega, \xi) + \frac{1}{2} \varphi_{\omega\omega} - \varphi \cos^2 \omega - |\varphi|^2 \varphi = 0, \quad 0 < \delta \leq 1, \quad (4.10)$$

with the initial condition

$$\varphi(\omega, 0) = \sin \omega, \quad (4.11)$$

where  $|\varphi|^2 = \varphi \bar{\varphi}$ ,  $\bar{\varphi}$  is the conjugate of  $\varphi$ , and the exact solution of (4.10) for  $\delta = 1$  is  $\varphi(\omega, \xi) = \sin(\omega) e^{\frac{-3i}{2}\xi}$ .

By performing Laplace transform (LT) on both sides of (4.10) and with the help of (4.11), we get

$$\mathcal{L}[\varphi(\omega, \xi)] = \frac{1}{s} [\sin \omega] + \frac{i}{\mathcal{A}(\delta)} \left( 1 - \delta + \frac{\delta}{s^{\delta}} \right) \mathcal{L} \left[ \frac{1}{2} \frac{\partial^2 \varphi}{\partial \omega^2} - \varphi \cos^2 \omega - \varphi \bar{\varphi} \varphi \right]. \quad (4.12)$$

The non-linear operator  $N$  is presented with the help of future algorithm as below

$$\begin{aligned} N[\Upsilon(\omega, \xi; q)] &= L[\varphi(\omega, \xi; q)] - \frac{1}{s} [\sin \omega] - \frac{i}{\mathcal{A}(\delta)} \left( 1 - \delta + \frac{\delta}{s^{\delta}} \right) \\ &\quad \times L \left[ \frac{1}{2} \frac{\partial^2 \varphi}{\partial \omega^2} - \varphi \cos^2 \omega - \varphi \bar{\varphi} \varphi \right]. \end{aligned} \quad (4.13)$$

The deformation equation of  $p^{th}$  order by the help of HATM at  $\mathcal{H}(\omega, \xi) = 1$ , is given as follows

$$\mathcal{L}[\varphi_p(\omega, \xi) - \chi_p \varphi_{p-1}(\omega, \xi)] = \hbar R_p(\vec{\varphi}_{p-1}, \omega, \xi), \quad (4.14)$$

where,

$$\begin{aligned} R_p(\vec{\varphi}_{p-1}, \omega, \xi) &= L[\varphi_{p-1}] - (1 - \chi_p) \frac{1}{s} (e^{i\mu\omega}) \\ &\quad - \frac{i}{\mathcal{A}(\delta)} \left( 1 - \delta + \frac{\delta}{s^{\delta}} \right) L \left[ \frac{1}{2} \frac{\partial^2 \varphi_{p-1}}{\partial \omega^2} - \varphi_{p-1} \cos^2 \omega - \sum_{r=0}^{p-1} \sum_{k=0}^r \varphi_k \bar{\varphi}_{k-r} \varphi_{p-r-1} \right]. \end{aligned} \quad (4.15)$$

On applying inverse LT to both side of (4.14), it reduces to

$$\varphi_p(\omega, \xi) = \chi_p \varphi_{p-1}(\omega, \xi) + \hbar \mathcal{L}^{-1} [R_p(\vec{\varphi}_{p-1}, \omega, \xi)]. \quad (4.16)$$



Table II: The absolute error analysis between proposed method and EADM [46] at  $\omega = 0.2$   $\delta = 1$ , and  $\hbar = -1$  for application 2.

$\xi$	Re $[\varphi]_{HATM}^{Abs}$	Re $[\varphi]_{EADM}^{Abs}$	Im $[\varphi]_{HATM}^{Abs}$	Im $[\varphi]_{EADM}^{Abs}$
0.1	$2.77556 \times 10^{-17}$	$2.77556 \times 10^{-17}$	$3.46945 \times 10^{-18}$	$3.46945 \times 10^{-18}$
0.2	$2.22045 \times 10^{-16}$	$2.22045 \times 10^{-16}$	0.00000	0.00000
0.3	$2.85605 \times 10^{-14}$	$2.85605 \times 10^{-14}$	$9.99201 \times 10^{-16}$	$9.99201 \times 10^{-16}$
0.4	$9.01057 \times 10^{-13}$	$9.01057 \times 10^{-13}$	$4.16195 \times 10^{-14}$	$4.16195 \times 10^{-14}$
0.5	$1.30975 \times 10^{-11}$	$1.30975 \times 10^{-11}$	$7.55923 \times 10^{-13}$	$7.55923 \times 10^{-13}$
0.6	$1.16620 \times 10^{-10}$	$1.16620 \times 10^{-10}$	$8.07848 \times 10^{-12}$	$8.07848 \times 10^{-12}$
0.7	$7.40353 \times 10^{-10}$	$7.40353 \times 10^{-10}$	$5.98459 \times 10^{-11}$	$5.98459 \times 10^{-11}$
0.8	$3.66893 \times 10^{-9}$	$3.66893 \times 10^{-9}$	$3.39027 \times 10^{-10}$	$3.39027 \times 10^{-10}$
0.9	$1.50474 \times 10^{-8}$	$1.50474 \times 10^{-8}$	$1.56469 \times 10^{-9}$	$1.56469 \times 10^{-9}$
1.0	$5.31541 \times 10^{-8}$	$5.31541 \times 10^{-8}$	$6.14324 \times 10^{-9}$	$6.14324 \times 10^{-9}$

On simplifying the above equation systematically by using initial condition (4.11), we can evaluate

$$\begin{aligned}
\varphi_0(\omega, \xi) &= \sin(\omega), \\
\varphi_1(\omega, \xi) &= -\hbar \left( \frac{-3i}{2} \right) \sin(\omega) \left( \frac{1 - \delta + \delta \left( \frac{\xi^\delta}{\Gamma(\delta+1)} \right)}{A(\delta)} \right), \\
\varphi_2(\omega, \xi) &= (1 + \hbar) \varphi_1(\omega, \xi) + \hbar^2 \left( \frac{-3i}{2} \right)^2 \sin(\omega) \frac{1}{(A(\delta))^2} \\
&\quad \times \left( 1 + 2\delta \left( 1 + \left( \frac{\xi^\delta}{\Gamma(\delta+1)} \right) \right) + \delta^2 \left( 1 + \left( \frac{\xi^{2\delta}}{\Gamma(2\delta+1)} \right) - 2 \left( \frac{\xi^\delta}{\Gamma(\delta+1)} \right) \right) \right),
\end{aligned}$$

Similarly, we obtain next terms in the same manner. The approximate solution of (4.10) for  $\hbar = -1$  and  $\delta = 1$  is given as:

$$\begin{aligned}
\varphi_M(\omega, \xi) &= \sum_{p=0}^M \varphi_p(\omega, \xi), \\
&= \sin(\omega) \left( 1 + \left( \frac{-3i}{2} \right) \xi + \left( \frac{-3i}{2} \right)^2 \frac{\xi^2}{2!} + \dots + \left( \frac{-3i}{2} \right)^M \frac{\xi^M}{M!} \right), \\
&= \sin(\omega) \sum_{p=0}^M \frac{\left( \frac{-3i}{2} \right)^p}{p!} \xi^p.
\end{aligned} \tag{4.17}$$

Letting  $M \rightarrow \infty$ , we have the exact solution of (4.1) as

$$\begin{aligned}
\varphi(\omega, \xi) &= \sin(\omega) \lim_{M \rightarrow \infty} \sum_{p=0}^M \frac{\left( \frac{-3i}{2} \right)^p}{p!} \xi^p, \\
&= \sin(\omega) e^{\frac{-3i}{2} \xi}.
\end{aligned} \tag{4.18}$$

## 5. Results and discussions

This section focuses on the numerical and graphical simulation of the Atangana-Baleanu-Caputo time-fractional NLSEs using the Laplace homotopy analysis method (LHAM). The primary advantage of the proposed algorithm lies in its ability to obtain both exact and approximate solutions in a straightforward manner without imposing any assumptions on the model. 2-D and 3-D graphs corresponding to various values of the fractional order  $\delta$  are plotted to illustrate the dynamic behavior of the considered equations. To highlight the simplicity and effectiveness of the proposed method, numerical comparisons and error analyses of the approximate solutions are presented. Tables I and II report the absolute errors between the approximate and exact solutions for the real and imaginary components of both applications. Figures 1 and 2 show the 3D plots of the fifth-order approximate solutions obtained via LHAM for different values of  $\delta = 0.7, 0.9, 1$  in application 1 with  $\Phi = 2$ ,  $\hbar = -1$ , and  $\mu = 1$ , along with their corresponding exact

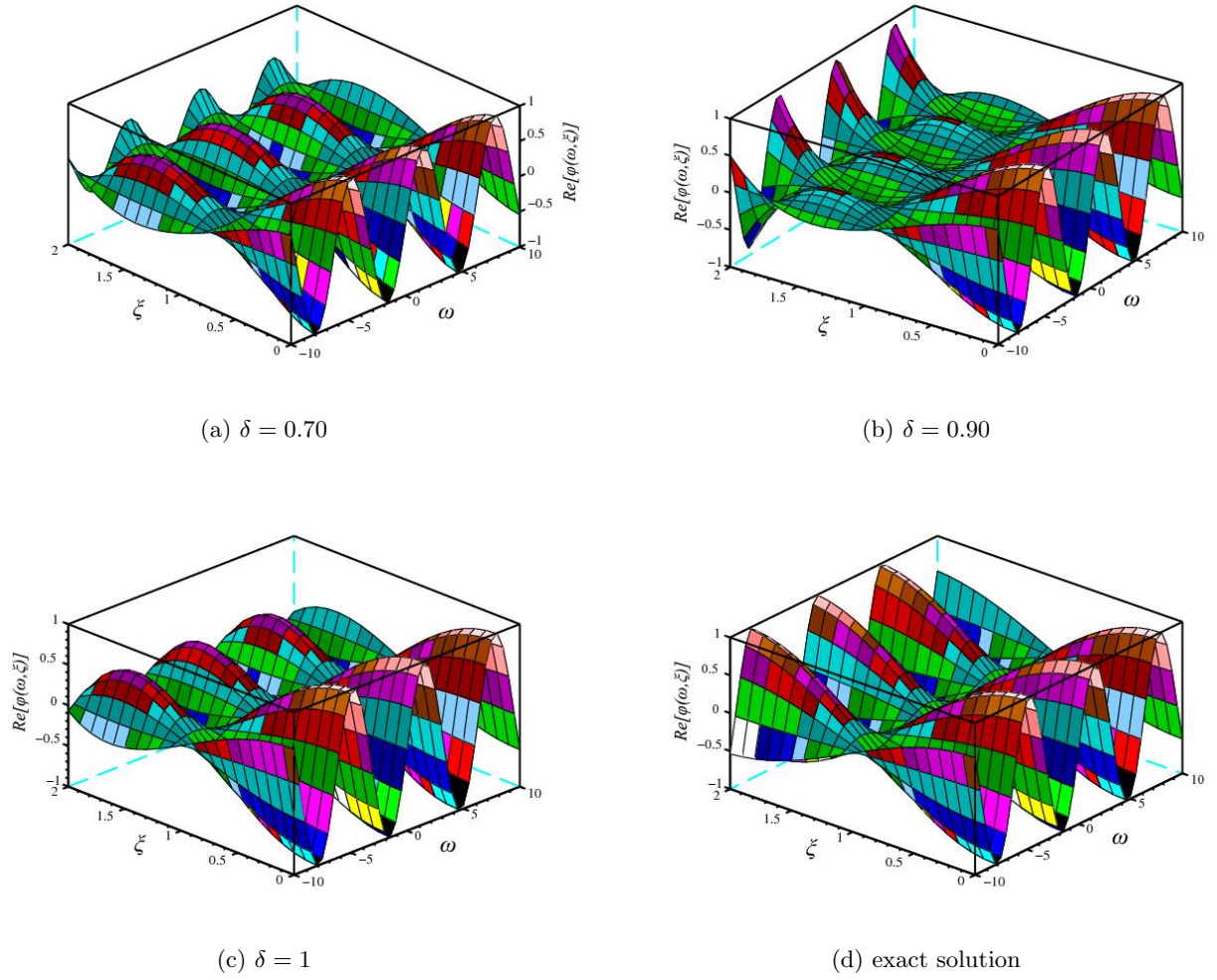
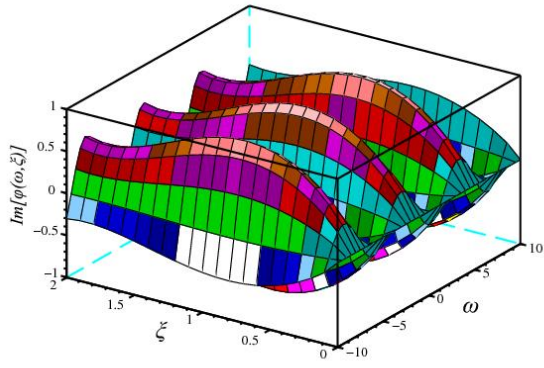
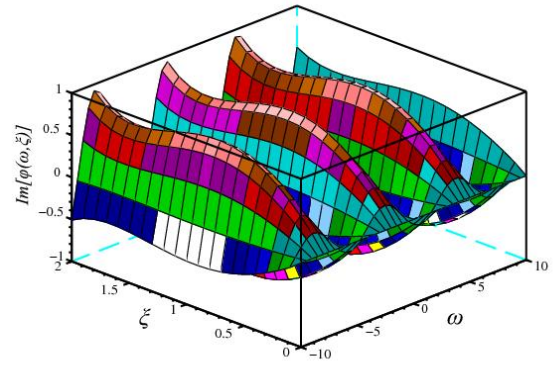
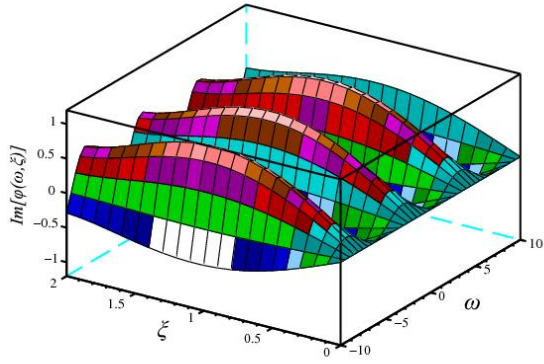
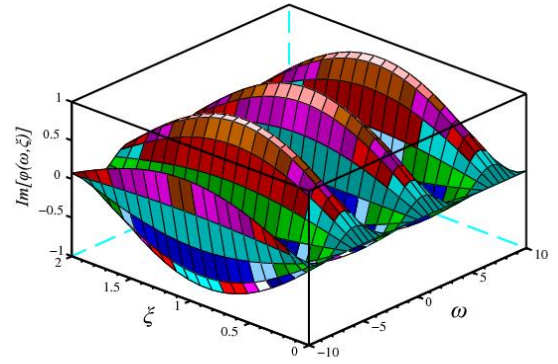
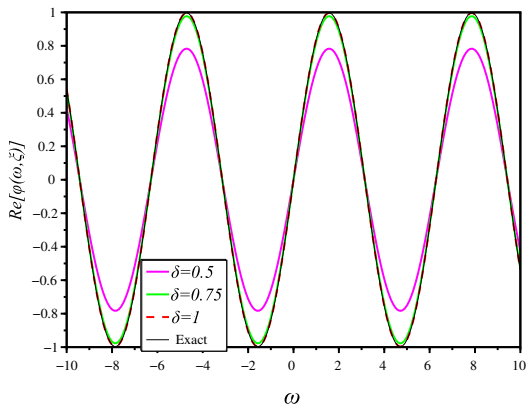


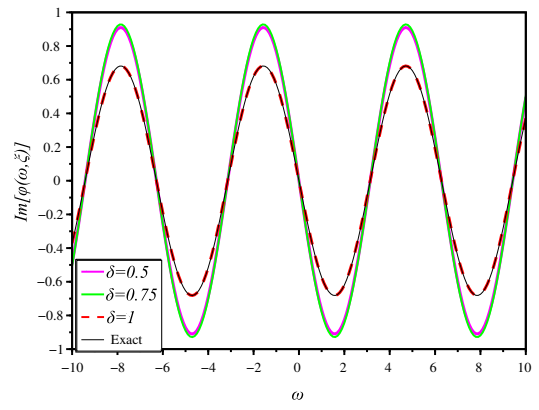
Figure 4: 3-D behaviour of real part of application 2 for various values of  $\delta$  with  $\hbar = -1$ .


 (a)  $\delta = 0.70$ 

 (b)  $\delta = 0.90$ 

 (c)  $\delta = 1$ 


(d) exact solution

 Figure 5: 3-D behaviour of the imaginary part of application 1 for various values of  $\delta$  with  $\hbar = -1$ .


(a) (a)



(b) (b)

 Figure 6: 2-D plots (a) real part and (b) imaginary part of application 2 for various values of  $\delta$  with  $\hbar = -1$ , and  $\xi = 0.3$ .

solutions. Similarly, figures 4 and 5 present the 3D plots for application 2 under the same values of  $\delta$  with  $\hbar = -1$ .

Figures 3 and 6 depict the effect of the variable  $\omega$  and the fractional derivative order  $\delta$  on the solution profiles by comparing the exact and approximate solutions. The 2D graphs in figures 3 and 6 display the fifth-order approximate solutions generated by LHAM at  $t = 0.5$  for  $\delta = 0.5, 0.75, 1$ , alongside the corresponding exact solutions for applications 1 and 2, respectively. These figures reveal that the accuracy of the approximate solutions improves as  $\delta \rightarrow 1$ , with a near-perfect match observed at  $\delta = 1$ , thereby validating the accuracy and reliability of the proposed technique. In conclusion, the graphical analysis confirms that the suggested method yields highly accurate series-form solutions with minimal computational burden.

## 6. Conclusions

This article introduces a hybrid iterative approach for solving NLSEs involving the Atangana-Baleanu fractional derivative. The proposed method combines the Laplace transform (LT) with the homotopy analysis method (HAM) to derive both approximate and exact analytical solutions for nonlinear fractional model. Key advantages of this technique include its simplicity in obtaining exact solutions for nonlinear fractional problems, reduced computational effort, reliance on the concept of limits, and the absence of assumptions about physical parameters. The effectiveness of the method is validated through numerical and graphical simulations, with results compared to established techniques such as the homotopy perturbation transform method (HPTM) and the Elzaki Adomian decomposition method (EADM). From the simulation perspective, the comparisons reveal that the proposed approach yields identical exact solutions to those obtained by the other methods. Additionally, 2D and 3D plots provide a clear physical interpretation of the behavior of the system for various values of the fractional order  $\delta$ . This article concludes that the Atangana-Baleanu derivative is well-suited for modeling the considered fractional differential equations, and that the Laplace homotopy analysis method (LHAM) offers a precise, adaptive, and efficient solution technique. Furthermore, this method holds potential for solving a wide range of fractional-order ordinary and partial differential equations. Future work may explore the application of the Laplace Fractional Residual Power Series (RPS) method to more complex systems of fractional partial differential equations across various scientific disciplines.

### Data Availability

No data were used to support this study.

### Conflicts of interest

There is no conflict of interest regarding the publication of this article.

### Funding

This study did not receive any funding in any form.

### Authors' contributions

The authors contributed equally and significantly in writing this paper. All authors read and approved the final manuscript.

### Acknowledgement

Not applicable.

## References

1. Arshad M., Seadawy A.R., and Lu D., *Modulation stability and dispersive optical soliton solutions of higher order nonlinear Schrödinger equation and its applications in mono-mode optical fibers*, Superlattices Microstruct. 113 (1), 419–429, (2018).
2. Kumar S., Kumar A., and Wazwaz A.M., *New exact solitary wave solutions of the strain wave equation in micro structured solids via the generalized exponential rational function method*, Eur. Phys. J. Plus 135, 870, (2020).
3. Yavuz M., Sulaiman T.A., Yusuf A., and Abdeljawad T., *The Schrödinger-KdV equation of fractional order with Mittag-Leffler nonsingular kernel*, Alex. Eng. J. 60 (2), 2715–2724, (2021).
4. Grinevich P.G., and Santini P.M., *The exact rogue wave recurrence in the NLS periodic setting via matched asymptotic expansions, for 1 and 2 unstable modes*, Phys. Lett. A 382, 973–979, (2018).
5. Chabchoub A., and Grimshaw R.H.J., *The hydrodynamic nonlinear Schrödinger equation: space and time*, Fluids 1, 23, (2016).

6. Mirzazadeh M., Akinyemi L., Senol M., and Hosseini K., *A variety of solitons to the sixth-order dispersive (3+1)-dimensional nonlinear time-fractional Schrödinger equation with cubic-quintic-septic nonlinearities*, Optik 241, 166318, (2021).
7. Khater M.M., Inc M., Attia R.A., Lu D., and Almohsen B., *Abundant new computational wave solutions of the GM- $DP$ -CH equation via two modified recent computational schemes*, J. Taibah Univ. Sci. 14 (1), 1554–1562, (2020).
8. Sahoo S., Ray S.S., Abdou M.A.M., Inc M., and Chu Y.M., *New soliton solutions of fractional Jaulent-Miodek system with symmetry analysis*, Symmetry 12 (6), 1001, (2020).
9. Rezazadeh H., Ullah N., Akinyemi L., Shah A., Mirhosseini-Alizamin S.M., and Chu Y.M., *Optical soliton solutions of the generalized non-autonomous nonlinear Schrödinger equations by the new Kudryashov's method*, Results Phys. 24, 104179, (2021).
10. Akbar M.A., Akinyemi L., Yao S.W., Jhangeer A., Rezazadeh H., and Khater M.M.A., *Soliton solutions to the Boussinesq equation through sine-Gordon method and Kudryashov method*, Results Phys. 25, 104228, (2021).
11. Yadav L.K., Agarwal G., Gour M.M., and Kumari M., *Analytical approach to study weakly nonlocal fractional Schrödinger equation via novel transform*, Int. J. Dynam. Control 12, 271–282, (2024).
12. Laskin N., *Fractional quantum mechanics*, Phys. Rev. E 62 (3), 3135, (2000).
13. Bardou F., Bouchaud J.P., Emile O., Aspect A., and Cohen-Tannoudji C., *Subrecoil laser cooling and Lévy flights*, Phys. Rev. Lett. 72 (2), 203, (1994).
14. Saubamea B., Leduc M., and Cohen-Tannoudji C., *Experimental investigation of nonergodic effects in subrecoil laser cooling*, Phys. Rev. Lett. 83 (19), 3796, (1999).
15. Atangana A., and Baleanu D., *New fractional derivatives with non-local and non-singular kernels: theory and application to heat transfer model*, Therm. Sci. 20, 763–769, (2016).
16. Hasan S., El-Ajou A., Hadid S., Al-Smadi M., and Momani S., *Atangana-Baleanu fractional framework of reproducing kernel technique in solving fractional population dynamics system*, Chaos Solit. Fract. 133, 109624, (2020).
17. Al-Smadi M., Dutta H., Hasan S., and Momani S., *On numerical approximation of Atangana-Baleanu-Caputo fractional integro-differential equations under uncertainty in Hilbert space*, Math. Model. Nat. Phenom. 16, 41, (2021).
18. Alaroud M., Ahmad R.R., and Din U.K.S., *An efficient analytical-numerical technique for handling model of fuzzy differential equations of fractional-order*, Filomat 33 (2), 617–632, (2019).
19. Alaroud M., Al-Smadi M., Ahmad R.R., and Din U.K.S., *An analytical numerical method for solving fuzzy fractional Volterra integro-differential equations*, Symmetry 11, 205, (2019).
20. Jleli M., Kumar S., Kumar R., and Samet B., *Analytical approach for time fractional wave equations in the sense of Yang-Abdel-Aty-Cattani via the homotopy perturbation transform method*, Alex. Eng. J. 59, 2859–2863, (2020).
21. Daniel Y.S., and Daniel S.K., *Effects of buoyancy and thermal radiation on MHD flow over a stretching porous sheet using homotopy analysis method*, Alex. Eng. J. 54 (3), 705–712, (2015).
22. Alhamzi G., Prasad J.G., Alkahtani B.S.T., and Dubey R.S., *Unveiling new insights: taming complex local fractional Burger equations with the local fractional Elzaki transform decomposition method*, Front. Appl. Math. Stat. 10, 1323759, (2024).
23. Alazman I., Mishra M.N., Alkahtani B.S., and Dubey R.S., *Analysis of infection and diffusion coefficient in an SIR model by using generalized fractional derivative*, Fractal Fract. 8 (9), 537, (2024).
24. Alazman I., Mishra M.N., Alkahtani B.S., and Goswami P., *Computational analysis of rabies and its solution by applying fractional operator*, Appl. Math. Sci. Eng. 32 (1), (2024).
25. Agarwal H., Mishra M.N., and Dubey R.S., *Exploring a mathematical model for the interaction between cancer cells and virotherapy utilizing fractional derivative*, Palestine J. Math. 14 (1), 694–706, (2025).
26. Yadav M.P., and Agarwal R., *Numerical investigation of fractional–fractal Boussinesq equation available to purchase*, Chaos 29, 013109, (2019).
27. Dubey R.S., Mishra M.N., and Goswami P., *Effect of Covid-19 in India – a prediction through mathematical modeling using Atangana–Baleanu fractional derivative*, J. Interdiscip. Math. 25 (8), 2431–2444, (2022).
28. Jafari H., Ganji R.M., Salati S., and Johnston S.J., *A mixed-method to numerical simulation of variable order stochastic advection diffusion equations*, Alexandria Eng. J. 89, 60–70, (2024).
29. Jafari H., Jassim H.K., Unlu C., and Vguyen V.T., *Laplace decomposition method for solving the two-dimensional diffusion problem in fractal heat transfer*, Fractals 32 (4), 2440026, (2024).
30. Yadav L.K., Gour M.M., Meena V.K., Bonyah E., and Purohit S.D., *Approximate analytical solutions of fractional coupled Whitham–Broer–Kaup equations via novel transform*, Int. J. Optim. Control Theor. Appl. 15 (1), 35–49, (2025).
31. Yadav S.K., Purohit M., Gour M.M., Yadav L.K., and Mishra M.N., *Hybrid technique for multi-dimensional fractional diffusion problems involving Caputo–Fabrizio derivative*, Int. J. Math. Ind. 16 (1), (2024).

32. Liao S.J., *The proposed homotopy analysis technique for the solution of nonlinear problems*, Ph.D. thesis, Shanghai Jiao Tong University, Shanghai, (1992).
33. Liao S.J., *An approximate solution technique not depending on small parameters: A special example*, Int. J. Non-Linear Mech. 30 (3), 371–380, (1995).
34. Liao S.J., *An optimal homotopy-analysis approach for strongly nonlinear differential equations*, Commun. Nonlinear Sci. Numer. Simul. 362, 2003–2016, (2010).
35. Elsaied A., *Homotopy analysis method for solving a class of fractional partial differential equations*, Commun. Nonlinear Sci. Numer. Simul. 16 (9), 3655–3664, (2011).
36. Van Gorder R.A., and Vajravelu K., *Analytical and numerical solutions to the Lane-Emden equation*, Phys. Lett. A 372, 6060–6065, (2008).
37. Bataineh A.S., Noorani M.S.M., and Hashim I., *Solutions of time-dependent Emden-Fowler type equations by homotopy analysis method*, Phys. Lett. A 371, 72–82, (2007).
38. Songxin L., and Jeffrey D.J., *Comparison of homotopy analysis method and homotopy perturbation method through an evolution equation*, Commun. Nonlinear Sci. Numer. Simul. 14 (12), 4057–4064, (2009).
39. Atangana A., and Baleanu D., *New fractional derivatives with nonlocal and non-singular kernel: Theory and application to heat transfer model*, Therm. Sci. 20 (2), 763–769, (2016).
40. Arshad M., Choi J., Mubeen S., Nisar K.S., and Rahman G., *A new extension of Mittag-Leffler function*, Commun. Korean Math. Soc. 33 (2), 549–560, (2018).
41. Caputo M., and Fabrizio M., *A new definition of fractional derivative without singular kernel*, Prog. Fract. Differ. Appl. 1 (2), 73–85, (2015).
42. Liaqat M.I., and Akgül A.A., *A novel approach for solving linear and nonlinear time-fractional Schrödinger equation*, Chaos Solit. Fract. 162, 112487, (2022).
43. Sadighi A., and Ganji D.D., *Analytic treatment of linear and nonlinear Schrödinger equations: a study with homotopy-perturbation and Adomian decomposition methods*, Phys. Lett. A 372 (4), 465–469, (2008).
44. Kanth A.R., and Aruna K., *Two-dimensional differential transform method for solving linear and non-linear Schrödinger equations*, Chaos Solit. Fract. 41 (5), 2277–2281, (2009).
45. Wazwaz A.M., *A study on linear and nonlinear Schrödinger equations by the variational iteration method*, Chaos Solit. Fract. 37 (4), 1136–1142, (2008).
46. Liaqat M.I., *A Hybrid Approach to Approximate and Exact Solutions for Linear and Nonlinear Fractional-Order Schrödinger Equations with Conformable Fractional Derivatives*, Electron. J. Appl. Math. 2 (3), 1–26, (2024).

Vijay Kumar Regar, Hoshiyar Singh,

Department of Mathematics,

Jaipur National University, Jaipur,

India.

E-mail address: Vijayjal7798@gmail.com

E-mail address: hoshiyar@jnujaipur.ac.in

and

Seema Verma,

Department of Computer Science & Engineering,

Vivekananda Global University, Jaipur,

India.

E-mail address: lokeshmanjeetyadav8@gmail.com

and

Ravi Shanker Dubey,

ASAS,

Amity University Rajasthan, Jaipur, India.

E-mail address: ravimath13@gmail.com